Orientation behaviour of crystallites in cylindrical polyethylene rods under tension–torsion combined stress

Takeshi Katagiri, Masanobu Sugimoto, Eiji Nakanishi* and Sadao Hibi
Department of Materials Science and Engineering, Nagoya Institute of Technology, Gokiso-cho, Showa-ku, Nagoya 466, Japan
(Received 6 December 1991; revised 27 April 1992)

A tension–torsion combined stress was loaded onto cylindrical rods of polyethylene to investigate the deformation mechanism of the crystalline phase under non-uniform stress. On applying the combined stress, a neck occurred at the centre of the sample and extended in the axial direction. After necking occurred, the twist deformation generated compressive stress in the radial direction, which suppressed the formation of micro-voids. Wide-angle X-ray diffraction revealed the following facts. The c axis, i.e. the crystal molecular chain axis, deviates from the axial direction owing to the combined loading of the tensile force and the shear force. The b axis, which is the long axis of the initial lamellae, orients selectively in the radial direction in the non-uniform stress state in which the shear stress increases in proportion to the distance from the centre of the cylindrical rod.

INTRODUCTION

It is very common to use polyethylene to study the deformation mechanism of crystalline polymers. Because of its complex supermolecular structure, the analyses have been carried out by various methods. As a foundational study, for example, twinning[1] and chain tilting[2] in a single crystal have been investigated. Rotation and twist of crystal lamellae and slippage between lamellae have been proposed to explain the deformation of the kink bands that occurred during the restretching of pre-oriented samples[3,4]. However, it is doubtful whether the above mechanisms can be properly applied to all polyethylene materials owing to the variation of deformation mode in the sample thickness direction[5]. Furthermore, the deformation modes used for the above analyses were for the case in which a uniform stress state could be assumed within a sample as the uniaxial tension or compression was applied. The deformation mechanism in the non-uniform stress state remains unknown.

We loaded high-density polyethylene cylindrical rods with a tension–torsion combined stress and studied the deformation mechanism under the non-uniform stress state. The shear stress increases in proportion to the distance from the central axis of the sample[6], which implies that the samples are deformed under a non-uniform stress state. The deformation mechanism in such a stress state has not yet been studied. As the shear stress acts efficiently for slip deformation of crystallites[7], it is expected that the analysed deformation mechanism

in such a stress state will give useful information on superdrawing of polymers. In this paper, the results of an investigation on the macroscopic deformation and the microscopic crystalline orientation of high-density polyethylene under the combined stress state are reported and discussed.

EXPERIMENTAL

Samples

High-density polyethylene Hizex 5300B ($M_w = 1.3 \times 10^5$) was supplied by Mitsui Petrochemical Industries Ltd. It had been moulded by an extruder to a cylindrical rod of 20 mm diameter. The material was further processed to the test specimen as shown in *Figure 1*. This shape prevents the chuck effect and induces a concentration of loading on the parallel part. Radial benchmarks at intervals of 90° and vertical benchmarks at intervals of 5 mm were placed on the sample surface.

Testing apparatus

The testing device used was a Tensilon UTM-5T (Orientec Co.) equipped with a twisting apparatus[8].

Combined stress loading

The tension–torsion combined loading was performed at $23 \pm 1°C$. Test conditions are summarized in *Table 1*. Macroscopic observations were made on the displacement λ between chucks, the tensile force F, the twist angle θ between chucks and the torsional torque T. During the test, photographs were taken to trace the change of the shape.

---

*To whom correspondence should be addressed

Table 1 Conditions of the combined stress loading experiments

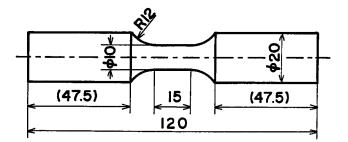| Notation	Tensile speed (mm min^{-1})	Torsional speed (deg min^{-1})
Tension	0.5	–
A	0.5	8
B	0.5	15
C	0.5	25
Torsion	–	15

Figure 1 Sample shape used in the combined stress loading
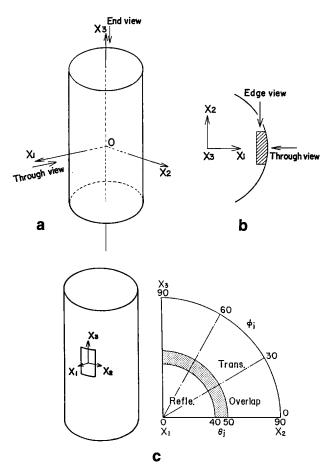

Figure 2 Cartesian coordinates O–$X_1X_2X_3$ for the X-ray diffraction analysis: (a) cylindrical sample; (b) outside block of a cylindrical sample; and (c) outside chip of a cylindrical sample

Density measurements

Density was measured using a density gradient column of carbon tetrachloride and methanol at $23 \pm 1°C$. Before the measurement, the test specimen was dried in a vacuum oven for 24 h.

WAXD photographs

Wide-angle X-ray diffractograms were taken using an X-ray generator (JDX-5P, Japan Electron Optics Laboratory Co.) equipped with an automatic diffracto-meter with Ni-filtered Cu Kα radiation. Test conditions were 36 kV and 13 mA with 4 h exposure time. Three types of test-pieces for X-ray diffraction were cut from deformed samples. The cylindrical bulk shown in *Figure 2a* was segmented in the cross-section perpendicular to the axial axis. The rectangular pieces were segmented from the central part of the sample and from the surface part. The coordinates of the test-piece were set as shown in *Figure 2b*.

Pole figures

The sample for pole figure analysis was prepared by slicing off the surface materials into chips 3 mm in length, 1 mm in width and 0.4 mm in thickness. These chips were then adhered by amorphous adhesive. A measurement technique similar to that applied for the case of a film was used. The equipment used was a Rigaku X-ray generator (CN2028) equipped with a pole figure attachment (PMG-A2). Tests were performed at 40 kV and 20 mA with Ni-filtered Cu Kα radiation. The scan speed was 2 deg min^{-1} and the scan angle ranged from 18° to 39°. As shown in *Figure 2c*, the radial axis (the X_1 axis) was set as one of the poles. Diffraction intensity measurements were made by the reflection method according to Schulz[9] in the low-angle region ($\theta_j = 0-50°$) and by the transmission method according to Decker[10] in the high-angle region ($\theta_j = 40-90°$). Corrections of the polarization factor, the shape factor, the absorption effect, the reflection effect and amorphous and air scatterings were made before the diffraction intensity curve of the crystalline area was obtained. Because of the overlap of $(0\,0\,1)_{mono}$, $(1\,1\,0)_{orth}$ and $(2\,0\,0)_{orth}$ in the diffraction intensity curve, peak separation was performed using the Pearson VII function[11] to obtain the individual diffraction curve of each plane. The intensity level adjustment was done in the overlapped area ($\theta_j = 40-50°$) of the reflection method and the transmission method for respective diffraction planes. Thus, after determining the diffraction intensity of planes of $(1\,1\,0)_{orth}$, $(2\,0\,0)_{orth}$ and $(0\,2\,0)_{orth}$, iso-intensity lines were drawn on the pole figures from the intensity of each diffraction plane in each θ_j and ϕ_j position.

RESULTS AND DISCUSSION

Deformation response

Bridgman[12] has studied the stress state of the necked area in a cylindrical rod under uniaxial tension. He suggested that the compressive stress in the radial direction towards the centre becomes larger as the radius of curvature in the necked area becomes smaller. It is clear that, when a material is deformed, the compressive force suppresses the formation of defects[13], and this is important in the application of the superdrawing technique.

Figure 3 shows photographs of neck formation in each combined stress loading. The necked area sizes were almost equal for all the conditions. As the twist deformation concentrated on the narrow necked area, the radius of curvature in the necked area became smaller as the twist became stronger. Whitening was also
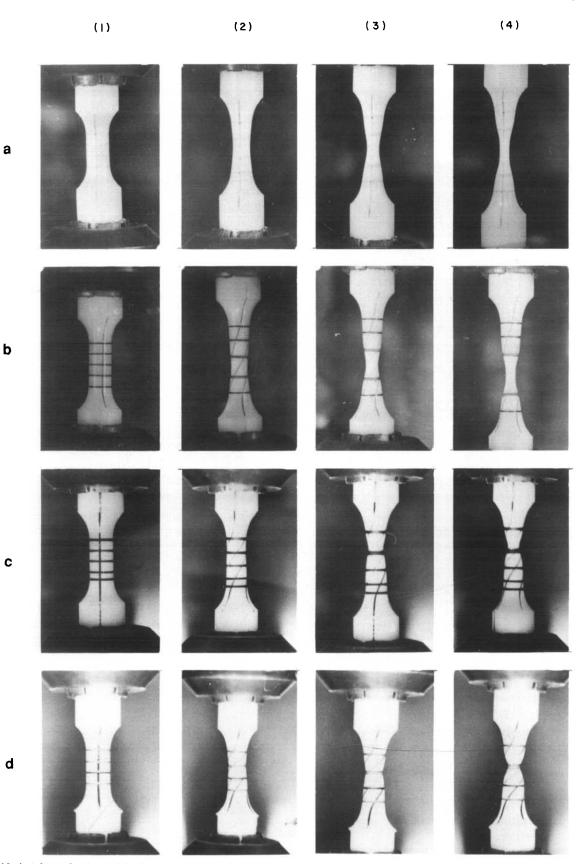
Figure 3 Neck deformation in combined stress loading, (1) before loading, (2) at neck initiation, (3) neck development and (4) neck completion: (a) tension; (b) condition A; (c) condition B; and (d) condition C

observed after necking propagated through the sample in the uniaxial tensile test. The draw ratio was determined from the premarked lines and is shown in *Table 2*. The ratio is not constant because of local deformation by necking. In a simple twist test, the draw ratio was set at

Table 2 Draw ratio of each sample loaded combined stress

	Tension	A	B	C	Torsion
Draw ratio	9.0	10.5	11.0	11.0	3.4

Table 3 Density of each sample loaded combined stress

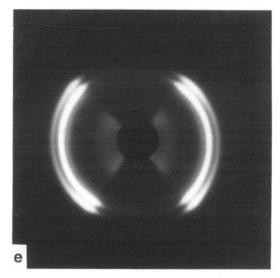|	Original	Tension	A	B	C	Torsion
Density	0.9518	0.9313	0.9432	0.9453	0.9460	0.9560

3.4 times, because buckling developed on strong twisting.

The results of density measurements are shown in *Table 3*. The generation of micro-voids is suppressed as the twist becomes stronger, as indicated by the fact that the reduction of density becomes smaller and whitening

Figure 4 Wide-angle X-ray diffraction through-view photographs of cylindrical samples loaded with combined stress: (a) original; (b) tension; (c) condition A; (d) condition B; and (e) condition C

is not noticeable after the neck has passed through the samples. In a simple twist test, where the gauge length in the axial direction was kept constant, a buckling phenomenon was observed. Buckling is interpreted as the suppression of extension in the axial direction. As no extension was allowed in the axial direction in the simple twist test, buckling was caused by the extension force resulting from the compressive stress in the sample radial direction. This suggests that the twist deformation generates a compressive stress along the radial direction and it suppresses micro-void generation on plastic deformation.
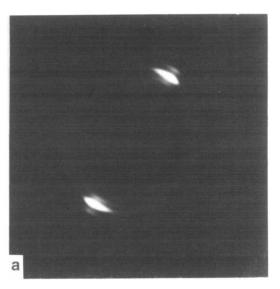
WAXD photographs

It is well known that the c axis, i.e. the molecular chain axis, orients preferentially in the drawing direction when polyethylene is highly stretched. We will discuss the unit-cell orientation for the case in which a tensile force and a shear force are simultaneously loaded onto the sample.

Figure 4 shows wide-angle X-ray diffraction photographs of cylindrical samples. Before deformation, it was almost in an unoriented state, as indicated by the uniform Debye–Scherrer rings on the through and the end view pictures. Attention is paid to the (1 1 0), (2 0 0) and (0 2 0) planes parallel to the c axis. For uniaxial drawn samples the diffractions from these planes appear as spots on the X_1–X_2 plane. However, for the combined stress loaded samples, the diffraction of each plane is split into two circular arcs with four maximum points that show symmetric intensity distribution to the X_1–X_2 plane (*Figures 4c, 4d* and *4e*). The acute angle formed by the diagonals connecting the maxima becomes larger as the twist becomes stronger.

Figure 5 shows the wide-angle X-ray diffraction photographs of thin plates cut out from the surface part (a) and the centre section (b) for the condition C. The intensity maxima of the (1 1 0), (2 0 0) and (0 2 0) reflections of the surface part deviate greatly from the X_1–X_2 plane, and their positions are equivalent to the intensity maxima of the circular arcs in *Figure 4e*. The diffraction from each plane of the centre section appears near the X_1–X_2 plane. This implies that the direction of the c axis deviates from the sample axis at the sample surface and is aligned with the sample axis at the central region. Here, at the sample surface, the angle between the sample axis and the c axis is defined as the spiral orientation angle.

In combined stress loading, the tensile force distributes uniformly in the cross-sectional plane and the shear force shows a distribution in proportion to the distance from the sample centre axis[6]. In other words, the resultant direction of the combined force tends towards a direction that is different from the sample axis in the cylindrical sample and this tilt angle is proportional to the distance from the sample axis. This indicates that the molecular chain axis also orients in a direction that is different from the sample axis. If the c axis orients along the resultant force, the tilt angle of the c axis from the sample axis will become larger as the distance from the centre becomes longer. The tilt angle should correspond to the angle between the line connecting spots of (1 1 0) and (2 0 0) planes and the X_1–X_2 plane in the X-ray photograph. This explains the different diffraction patterns under various test conditions. It should be
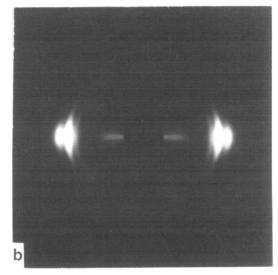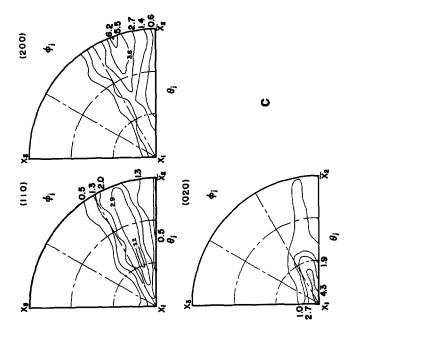

Figure 5 Wide-angle X-ray diffraction photographs of cylindrical samples loaded with combined stress in condition C: (a) outside block; and (b) centre block
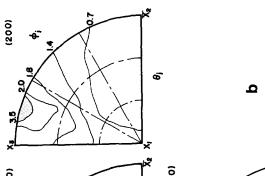
remembered that the diffraction patterns in *Figure 4* were taken from cylindrical rods. Thus, each of them is a composite of diffractions from different sample portions, and includes not only the patterns (a) and (b) in *Figure 5*, but also those patterns in between them. This is the reason why circular arcs are observed in *Figure 4*. These results reveal that the crystalline molecular chains orient along the resultant force of the combined tensile and shear forces.
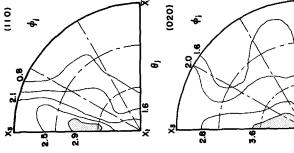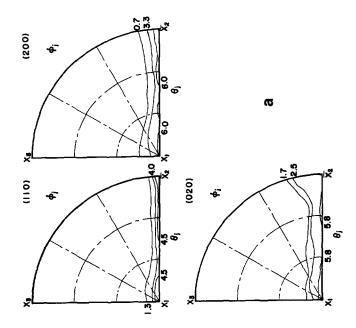
Pole figures

Kasai *et al.*[14] have studied the crystal orientation in detail during neck formation in polyethylene rods under uniaxial tension. They concluded that, after the completion of necking, the c axis is oriented in the axial direction, while the a and b axes showed random orientation in the plane perpendicular to the draw axis. We have discussed the orientation behaviour of the c axis above in the case of a combined stress deformation. The orientation of the a and b axes will be discussed below.
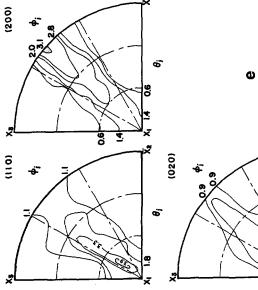
Figure 6 shows the pole figures obtained by wide-angle X-ray diffraction. The normal vectors of (1 1 0), (2 0 0) and (0 2 0) planes in the pole figures of a uniaxially tensile

Figure 6 Pole figures of the sample loaded with combined stress: (a) tension; (b) torsion; (c) condition A; (d) condition B; and (e) condition C
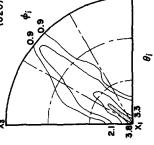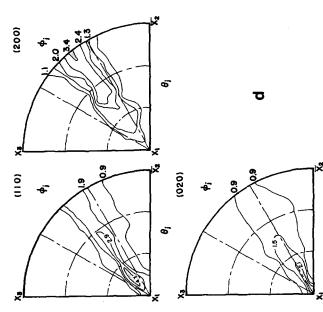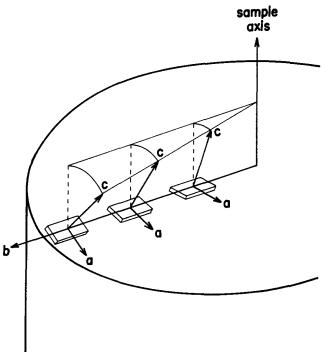
sample
axis

Figure 7 Schematic representation of the orientation behaviour of crystalline blocks in a deformed polyethylene rod under combined stresses

deformed sample in *Figure 6a* are distributed randomly on the X_1-X_2 plane and do not show any concentration of a peak. This means that the a and b axes orient randomly in the plane perpendicular to the sample axis. *Figure 6b* shows the pole figure of a simply twisted sample. No selective orientation of the (1 1 0), (2 0 0) and (0 2 0) planes is observed in the uniaxial tensile test. In the case of a simple twist test, with 3.4 times twisting, the normal vector of the (0 2 0) plane orients in the X_1 direction. Thus, it is suggested that non-uniform stress due to the distribution of shear stress in the X_1-X_2 plane is the reason for the different orientation behaviour of the crystallites as observed above. *Figures 6c, 6d* and *6e* are the pole figures of combined stress deformed samples. The normal vectors of the (1 1 0), (2 0 0) and (0 2 0) planes are distributed in a plane that is only azimuthally rotated from the X_1-X_2 plane. This means that the c axis, which is perpendicular to the normal of (1 1 0), (2 0 0) and (0 2 0) planes, orients strongly in the direction that is only azimuthally rotated from the sample axial direction. This azimuthal angle ϕ_j agrees with the spiral orientation angle obtained by wide-angle X-ray diffraction photographs. The (0 2 0) plane normal vector, which denotes the b axis, orients selectively in the X_1 axial direction, which corresponds to the radial direction. The (2 0 0) plane normal vector, which denotes the a axis, is oriented selectively in the X_2 direction, which is the sample circumferential direction. From the results of *Figures 4* and *6*, the orientation behaviour of segmented crystalline blocks can be presented schematically as shown in *Figure 7*.

The angle between the (1 1 0) plane normal vector and the b axis is 33.7° according to the unit cell of polyethylene[15]. In the condition A the (1 1 0) plane normal orients in a direction that deviates more than 30° from the (0 2 0) plane normal, which corresponds to the b axis. While in the conditions B and C, the (1 1 0) plane normal orients in a direction less than 30° away from the b axis. In addition, the intensity maxima of the (1 1 0), (2 0 0) and (0 2 0) reflections for the conditions B and C become broad compared with that of the condition A. For the conditions B and C in which twisting is strong, the intensity maxima of the (1 1 0) plane normal shifts to the lower polar-angle side and spreads in the direction perpendicular to the c axis. It is thus suggested that the interlamellae slip deformation occurs due to the action of twisting. This deformation is just like a rotation around the c axis. The slip plane is likely to be the (1 1 0) plane because the (1 1 0) plane is the most atomic close-packed plane. This will be reported in detail in the next paper.

CONCLUSIONS

From the above results and discussion, the following conclusions are obtained.

Twisting generates a compressive stress towards the sample radial direction so that the occurrence of micro-voids is suppressed.

The crystal c axis, which is the molecular chain axis in the crystalline phase, orients in a direction that is different from the axial direction owing to the resultant force of the combined tensile and shear forces.

The crystal b axis, i.e. the initial lamellae major axis, orients selectively in the sample radial direction when deformed by the non-uniform stress state, in which the shear stress increases in proportion to the distance from the sample centre axis.

REFERENCES

1   Kiho, M., Peterlin, A. and Geil, P. H. *J. Appl. Phys.* 1964, **35**, 1519
2   Peterlin, A. *J. Polym. Sci.* (*C*) 1966, **15**, 427
3   Shigematsu, K., Imada, K. and Takayanagi, M. *J. Polym. Sci.* 1975, **13**, 73
4   Ginzburg, B. M., Sultanov, N. and Rashidov, D. *J. Macromol. Sci.-Phys.* (*B*) 1974, **9**(4), 609
5   Neki, K. and Geil, P. H. *J. Macromol. Sci.-Phys.* (*B*) 1974, **9**(1), 71
6   Gaydon, F. A. *Q. J. Mech. Appl. Math.* 1951, **5**, 29
7   Torii, T., Sumita, K., Hibi, S., Nakanishi, E., Maeda, M. and Fujimoto, K. *Kobunshi Ronbunshu* 1987, **44**(5), 331
8   Hibi, S., Katagiri, T., Ando, T., Noda, E., Maeda, M. and Nakanishi, E. *Kobunshi Ronbunshu* 1988, **45**(9), 713
9   Schulz, L. G. *J. Appl. Phys.* 1949, **20**, 1030
10   Decker, B. F., Aspand, B. T. and Harker, D. *J. Appl. Phys.* 1948, **19**, 388
11   Heuvel, H. M., Huisman, R. and Lind, K. C. J. B. *J. Polym. Phys.* 1976, **14**, 921
12   Bridgman, P. W. *Trans. Am. Soc. Met.* 1943, **32**, 553
13   Kamiya, T. and Yazaki, K. *Sen-i Gakkaishi* 1982, **38**, 20
14   Kasai, N. and Kakudo, M. *J. Polym. Sci.* (*A*) 1964, **2**, 1955
15   Swan, P. R. *J. Polym. Sci.* 1962, **56**, 409